Fractal river networks of Southern Africa

Jacek Stankiewicz
(corresponding author)
CIGCES, Department of Geology, University of Cape Town, Rondebosch 7701, South Africa
jacek@cigces.uct.ac.za

Maarten J. de Wit
CIGCES, Department of Geology, University of Cape Town, Rondebosch 7701, South Africa
maarten@cigces.uct.ac.za

ABSTRACT

Fractals and scaling laws abound in nature, and it is said that geometry of river networks and basins is an epitome of this. This study investigates how, in the southern section of the tectonically unique African continent, scaling parameters and deviations from 'perfect fractal patterns' relate to parameters like geomorphology through which the river flows, and the underlying geology. A number of river network scaling laws and scaling parameters have been put forward, but it has been suggested that all river networks can be divided into universality classes represented by just 2 of these scaling parameters. One of these is the fractal dimension of individual streams, usually labelled d and having a value of ~1.1. The other parameter, Hack's exponent h, expresses the dependence of stream length (l) on drainage area (a) via Hack's Law $l = ca^h$. There is no universal value for h. Different networks often have different values for h, and inside a given network the parameter is often observed to change with scale. We use the natural laboratory of networks in southern Africa to investigate the variations in Hack's exponent and find evidence to confirm the existence of scaling regimes. We attempt to explain these variations in scaling using the regime model of Dodds and Rothman (2000). At the smallest scale we find that non-convergent mountain streams exist in different settings, but their spacing is determined by underlying rock type. In this type of drainage $a \sim l$, and hence $h \approx 1$. Once streams begin to converge, the value of h drops, and is inversely correlated to the roughness of the underlying topography. This trend stops once basin sizes reach a threshold value, above which basins may be self-similar. This threshold varies in individual networks. In the smoothest topographies it occurs as low as 400 km^2, but can occur as high as 1400 km^2 in other networks. While we have identified a number of guidelines for correlating scaling parameters with basin settings, there exist significant variations around these guidelines which we can only attribute to randomness, or small variations in the initial conditions during the initial formation of the river basins.

Introduction

One possible way of studying geometry of river networks is by treating these networks as fractal structures, using scaling laws that we now know characterize fractals. A number of such laws have been put forward to show how various network parameters vary with scale. Such network studies often become very theoretical, and may involve unrealistic assumptions as their starting points. Shreve (1967) is an example of such studies – he assumes river networks to be infinite, as well as an absence of geological controls on their courses. Other studies (*e.g.* Maritan *et al.*, 1996; Rigon *et al.*, 1996) use relatively advanced mathematics, but do not present any conclusions regarding the geology and geomorphology in the river basins concerned. It is not our intention to criticise such papers – they are undoubtedly of value in topology, and provide us with a framework to look at river basins from a different angle. Indeed, we have recently published an article dealing strictly with the mathematical properties of river networks in southern Africa (Stankiewicz and de Wit, 2005). However, we feel that a study investigating how simple river network scaling laws and parameters controlling these depend on not only scale, but also local conditions such as underlying geology, geomorphology and climate, without extensive mathematical background, would be of use. We therefore begin by introducing the river basins of southern Africa, and follow that by describing basic scaling laws.

Data

Rivers of southern Africa provide an excellent natural laboratory for studying river networks. Drainage in the region is shown in Figure 1. The major river is the Orange, which is the 5th largest river in Africa both in terms of main stream length (2150 km) and drainage area (1,040,000 km^2). Its tributaries drain vastly different geological and climatic terrains. The upper Orange and Vaal sources are in the high ground inland of the Drakensberg Escarpment. This highland (reaching 3482 metres above sea level) has been suggested to be inherited from a deep mantle plume that brought about the break-up of Gondwana ~180 Ma (White and McKenzie, 1989). The fact that the Orange has its sources just 150 km west from the Indian Ocean, but flows to the Atlantic 1400 km away, has been seen as a case of drainage away from the new (Indian) Ocean, supporting the plume hypothesis (Cox, 1989).

The Molopo and Nossob rivers drain (technically speaking) the Kalahari basin. While presence of river terraces indicates both these rivers were once perennial

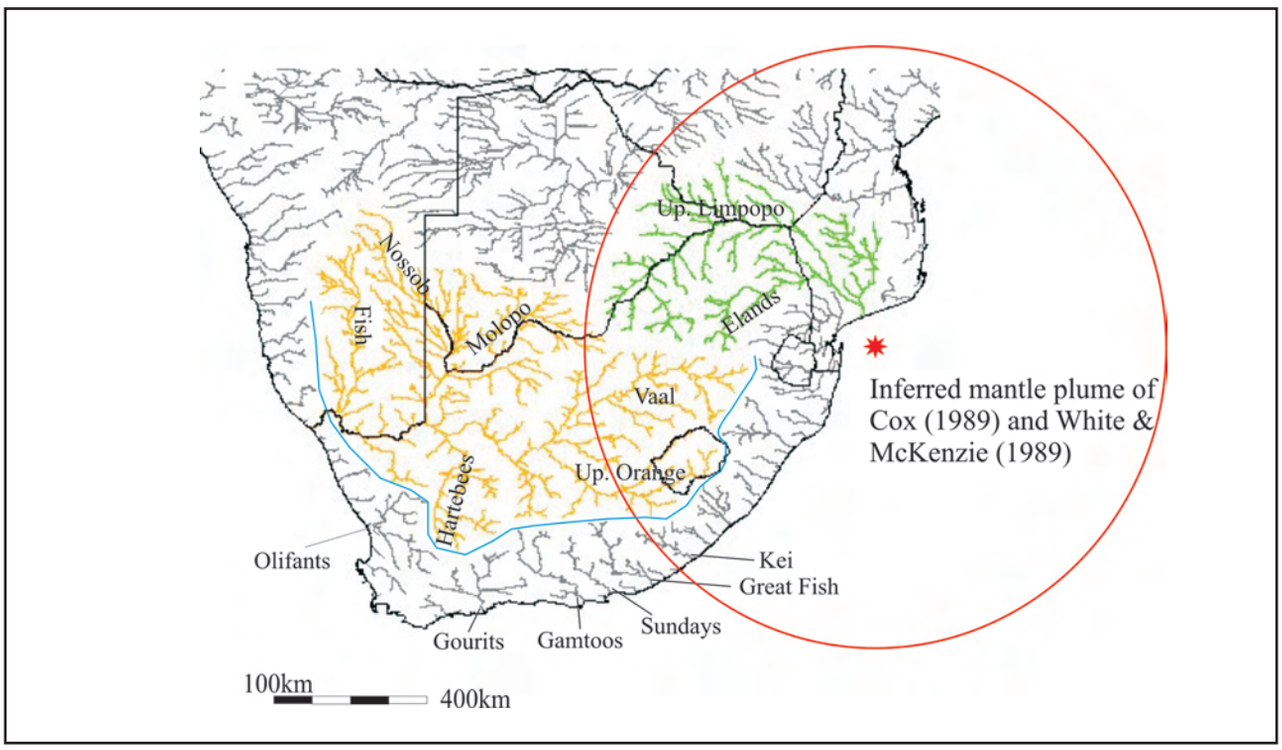

Figure 1. Drainage of Southern Africa. Orange River marked in orange, Limpopo in green. Their major sub-basins, as well as six main Cape Fold Belt rivers have been labelled. The Great Escarpment is marked in blue. The centre and radius of the inferred ~180 Ma mantle plume of Cox (1989) and White and McKenzie (1989) shown in red.

(de Wit, 1993), neither network has a record of permanent flow during living human history (Bootsman, 1997). When water is transported in the channels, overland flow never reaches the Orange – transport takes place by groundwater.

The Fish River flows south through the arid Namibia, and the only perennial section of its network is the channel a few kilometres upstream from its confluence with the Orange. The most dramatic feature of this river is the famous Fish River Canyon in the river's lower reaches. There the river has cut into the horizontal quartzitic sandstones and shales of the Nama Group (700 to 500 Ma) to reach the underlying schist and granite gneiss of the Namaqua Complex (1200 to 1000 Ma; Buckle, 1978). In places the canyon is over 500 metres deep.

Another major tributary of the Orange is the Hartebees, also known as the Sak. This river is also non-perennial, but fossil evidence indicates that as recently as 10 Ma the river flowed through a wet and wooded environment (de Wit, 1993).

The western, southern and eastern boundaries of the Orange River basin are formed by one of the main features of the region's geomorphology – the Great Escarpment (Figure 1). This divide stretches from southern Namibia to the Limpopo basin in an arc ~200 km from the coast, and is only breached by the antecedent gorge of the Orange just before its outlet. The divide is most spectacular in the Drakensberg on the South Africa – Lesotho border. The zone between the escarpment and the coast is drained by rivers

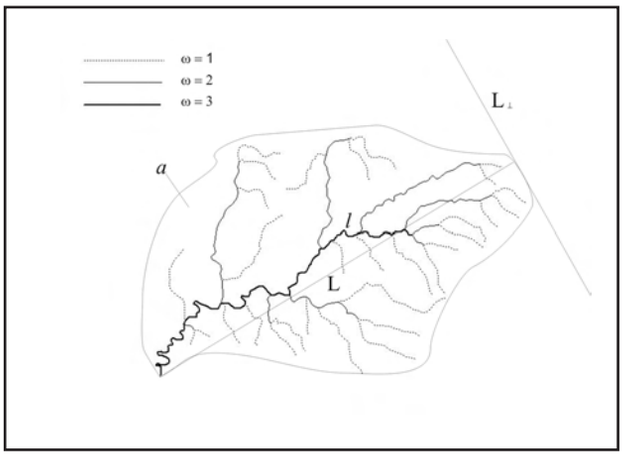

Figure 2. The Horton-Strachler ordering scheme for river networks and parameters commonly used in scaling laws. The legend shows what lines are used to represent orders 1, 2 and 3.

approximately perpendicular to the divide. Of these 6 are of particular interest: the Olifants, Gourits, Gamtoos, Sundays, Great Fish and Kei (Figure 1) cross a band of exhumed folded mountain ranges knows collectively as the Cape Fold Belt. These ranges have been extensively faulted and folded at ~250 Ma (*i.e.* before the break-up of Gondwana), and a trellis river pattern has developed across them. Main river segments have formed in the weaker shales, leaving the hard Table Mountain Sandstones (often quartzites) as vertical ridges. Lower order streams then flow down these steep ridges to join the main (higher order) stream. This environment is not

found anywhere else in southern Africa, hence our interest in it.

Another major river network in southern Africa is the Limpopo, which flows east forming the border between South Africa and Zimbabwe, before reaching the Indian Ocean through a delta in Moçambique. Cox (1989) suggests the Limpopo valley is a rift-inherited, related to the failed spreading axis in the Kalahari identified by Reeves (1972, 1978). The presence of this rift is consistent with the plume theory of White and McKenzie (1989).

For computational purposes, we used a 1 km horizontal resolution Digital Elevation Model (DEM) of the area. For sections of this study where this resolution was too coarse, 1:250,000 topographic maps were used.

Methods

Scaling laws of river networks

The first tool usually applied when studying a river network is stream ordering. The most common ordering scheme is the Horton-Strachler method (Figure 2), developed by Horton (1945) and later improved by Strachler (1957). In this scheme all source stream segments have order $\omega = 1$. When two source streams meet, the segment downstream from the junction has $\omega = 2$. The order increases by 1 when a stream joins another stream of the same order; when two streams of different orders meet, the segment downstream is assigned the higher of the two orders. Natural quantities to measure in an ordered basin are:

- the number of streams of a given order: $n(\omega)$,
- average length of streams of a given order: $l(\omega)$,
- average drainage area (enclosed by the watershed) of streams of each order: $a(\omega)$.

The outlet of the network obviously has the highest order in the system, and is labelled Ω. Clearly $n(\Omega) = 1$, and $a(\Omega)$ is the network's total drainage area.

Horton (1945) introduced a number of measurements that follow the ordering scheme discussed above. The first was the bifurcation ratio, $R_n(\omega)$, defined as the ratio of streams of order ω to ones of order $\omega+1$, *i.e.*

$$R_n(\omega) = \frac{n(\omega)}{n(\omega+1)} \tag{1a}$$

His suggestion that R_n is independent of w was the first scaling law in the study of river networks. Two more ratios can be defined:

$$R_l(\omega) = \frac{l(\omega+1)}{l(\omega)} \tag{1b}$$

$$R_a(\omega) = \frac{a(\omega+1)}{a(\omega)} \tag{1c}$$

Horton's laws state that the three ratios are independent of order. Note the three ratios are defined in such a way that they are all greater than unity.

One of the most famous scaling laws for river networks is Hack's law (Hack, 1957), which relates the main stream length (longest possible stream length from source to outlet) to its drainage area by the relation

$$l = ca^h \tag{2}$$

It could be expected from simple geometry that $a \sim l^2$, and therefore $h = 1/2$. However, in real networks different values of h are observed, usually $h \neq 1/2$. Hack found the exponent equal to 0.6, but noted fluctuations from basin to basin, with some of them having h as high as 0.7. Further studies (*e.g.* Rigon *et al.*, 1996; Maritan *et al.*, 1996) found h typically in the range (0.55, 0.60). A theoretical approach by Rigon *et al.* (1998) produces a value of $h = 0.57$ for what they term "feasible optimum" of the network. Furthermore, observed values for this exponent vary not just from basin to basin, but also with scale in a given network. Mueller (1973) identified three regimes where with $h = 0.6$ at the smallest scale, 0.5 at the intermediate (20,000 – 250,000 km^2) and 0.466 for the largest basins. More recently, in a theoretical study Dodds and Rothman (2000) conjectured the existence of up to 4 scaling regimes, with Hack's Law existing with a different exponent in each. The smallest basins belong to non-convergent streams running down hill slopes in parallel channels where, provided basins have a uniform width, $l \sim a$, and thus h has a value close to 1. When streams begin to converge, a decrease in h would be observed. Dodds and Rothman (2000) termed this the short-range regime. At even larger scales the authors note that correlations in stream and basin shape decrease, suggesting at this scale streams belong to a random regime, with yet another value for the exponent. Eventually, basins reach shapes constrained by continental-scale structures (maximal basins). As our study deals with drainage of a sub-continent, we will not deal with the last regime, but one of our aims is to test for the existence of these regimes, and attempt to specify their ranges and the values of h inside different regimes in different networks. However, other network parameters must first be introduced.

Two parameters are used to describe the actual shape of the basin: $L_{\parallel}$, the length of the basin parallel to the main stream, and $L_{\perp}$, the width of the basin (Figure 2). As $L_{\parallel}$ is used far more often it is usually written as just L. This convention can be confusing (as by default $l > L$), but we will persist with it. As with l, L can be related to the drainage area (Maritan *et al*, 1996)

$$a \sim L^D \tag{3}$$

The exponent D shows how basin area changes with different values of L, and is found in nature to have a value very close to 2. It can be thought of as the fractal dimension of the network, with $D = 2$ being a necessary and sufficient requirement for a network to be self-similar (*e.g.* Dodds and Rothman, 1999).

It is also possible to relate L, the basin length, and l, the stream length (*e.g.* Maritan *et al.*, 1996)

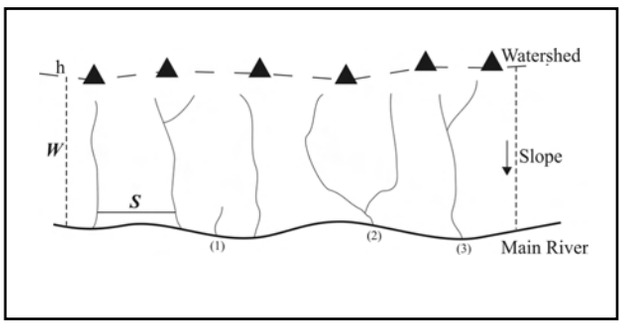

Figure 3. Schematic linear drainage studied to examine the hill-slope regime. Separation of adjacent streams (*S*) was measured here, as well as mountain slope, and, where possible, belt half-width (*W*) and the belts mean height above the mountain front. Streams starting less than halfway up the mountainside were not considered (1). When streams join before reaching the mountain front, they were counted as two if the confluence was in the lower half of the slope (2), otherwise the resulting stream was treated as one (3).

$$l \sim L^d \tag{4}$$

d, the parameter in this relation can be thought of as fractality of individual streams, and is usually observed to have a value between 1 and 1.2 for real networks. Note that the last three scaling parameters can be expressed in terms of each other: $D = d/h$.

For our purposes here, these equations suffice to quantify a network in terms of scaling parameters. Readers for who this is not sufficient are referred to the book of Rodriguez-Iturbe and Rinaldo (1997), and the references therein. As we stated in the introduction, we want to keep the mathematics to a minimum in this article.

Obtaining steams and networks from our datasets

River networks were constructed by computer simulations of water flow over the 1 km resolution Digital Elevation Model (DEM) of southern Africa. No differentiation was made between perennial and non-perennial streams, or even dry beds. All channels picked up in the DEM were treated as stream segments. As lengths of first order streams could not be uniquely determined, only orders from 2 upwards were included in the analysis. A detailed description of the process of generating such networks is provided by Stankiewicz (2004).

As this resolution was not enough to study the hill-slope regime postulated by Dodds and Rothman (2000), 1:250,000 topographic maps were used for that. It was mentioned earlier that parallel basins need to have equal width to belong to the $h \approx 1$ regime. The best setting for a study of parallel streams is the slope of a linear mountain belt. Thus once such regions were identified, we proceeded to measure the separation of such streams, which corresponds to basin width. This distance could be determined on the maps to the nearest 1 mm, which corresponds to 250 m. Interpretative ambiguities may arise with streams draining the mountainside converging before reaching the mountain front. In this study streams that joined up before flowing halfway down the slope were taken as one stream, while streams with sources less than halfway up the mountain slope were not considered at all (Figure 3).

Quantifying the topography

Just like river networks, topography can also be described as a fractal. To do that, it is necessary to think of elevation as a function of two co-ordinates: latitude and longitude. A fundamental consideration is the correlation between the elevation values at two points as a function of the distance between these points. As this distance increases, the less one would expect the elevation to be correlated. The mathematics involved in computing the fractal dimension of topography is rather complicated, and only a summary of the method of Turcotte (1992) will be presented here.

Consider an $N * N$ grid consisting of N^2 equally spaced points, each having a particular elevation $e(x,y)$. A two-dimensional discrete Fourier transform of this array will produce an $N * N$ grid of complex coefficients. Each of these coefficients is then assigned a radial wave number, corresponding to its position from a specified reference point in the grid, rounded to the nearest integer value. The two-dimensional mean power spectrum density is then defined as the mean of the squares of absolute values of all complex coefficients with the same wave number. The mean slope of the logarithmic plot of this power spectrum density as a function of the wave number then corresponds to the fractal dimension of the topography.

Turcotte (1992) noted that this fractal dimension is an insensitive measure of the topography. He found a much more descriptive parameter in the y-intercept of the above regression, which he showed is a measure of the roughness of the topography. He also showed that best-defined spectra are obtained when using grids with $N = 32$. In this study the dimension and roughness of a certain section of the landscape the 1 km DEM was used. An $m * n$ grid was first selected in such a way that both m and n were multiples of 32, and the relevant section was in the centre of the grid. The grid was then divided into 32 * 32 sub-grids, and dimension and roughness computed for each grid containing a section of the network. These were then averaged to give the values for the area concerned.

Analysis

Horton's ratios

Once the networks were computed from the DEM, the streams were ordered according to the Horton-Strachler scheme. The Orange was found to have $\Omega = 8$, the Limpopo $\Omega = 7$, and the six Cape Fold Belt networks each had Ω of either 5 or 6. Table 1 shows the values of stream number, lengths and areas for each order, as well as the corresponding Horton's ratios in each network.

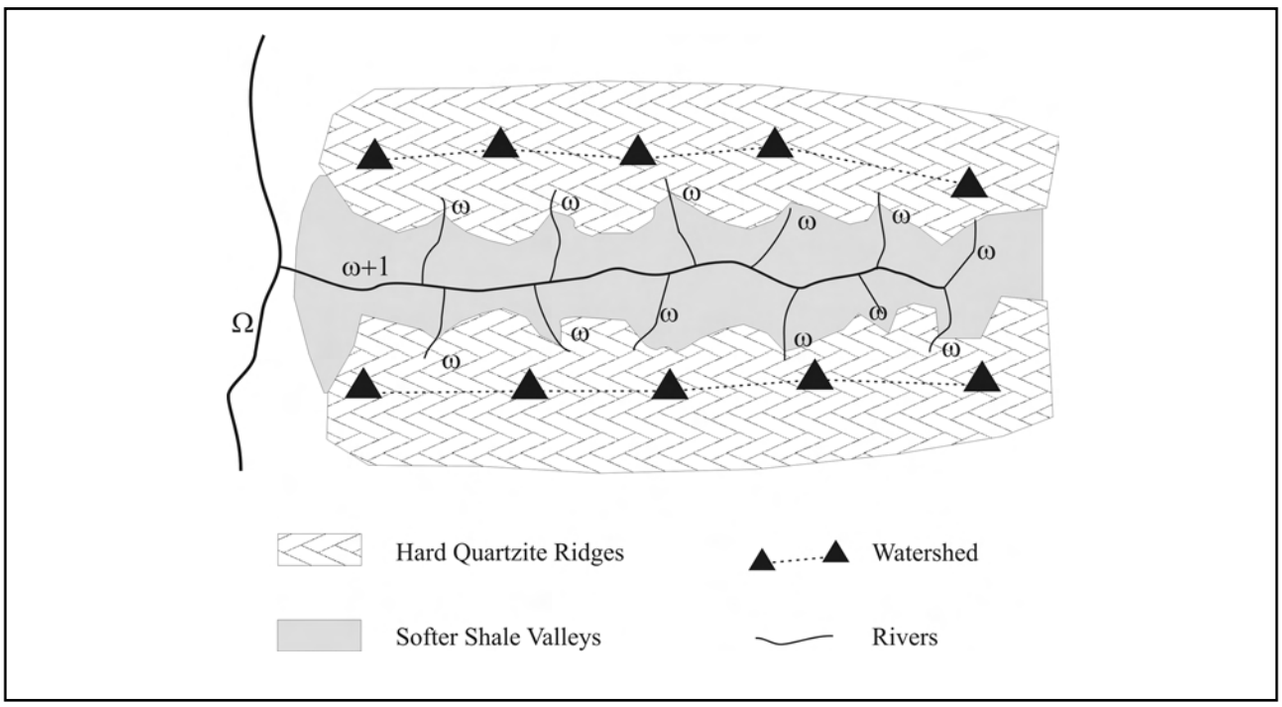

Figure 4. Schematic drainage of the parallel ridges of the Cape Fold Belt. Parallel low order streams (ω) drain the mountain side, reaching the trunk river (ω+1) flowing in the softer shale valley. Such drainage can cause apparent anomalies in Horton' ratios.

While it is obvious there deviations in Horton's ratios, some patterns can be observed in the Orange and Limpopo networks. R_l is always the smallest of the ratios, fluctuating between 1.5 and 3. At smaller orders the values of each ratio decrease with increasing order. At higher orders discrepancies can be attributed to having much fewer data points.

The Cape Fold Belt rivers are much smaller than the Limpopo, and hardly comparable to the Orange. With basin areas between 20,000 and 70,000 km^2, they can supply us with much less data, but not necessarily less insight – some interesting analyses can be performed. From Table 1 it is clear that there is considerably more variation in the ratio than was the case for the Orange, or even the Limpopo. In the Gamtoos basin R_n is as high as 8.50. Similarly, R_a is very high (>10 in two cases). These anomalies can be partially attributed to less data points available, but could also be a reflection of a real phenomenon. If a trunk stream flows through a soft shale valley with lower order streams draining the hard quartzite mountainsides on either side of the valley, the branching ratios can be affected, and Horton's ratio R_n will be larger than usual. There would, in fact, be a direct relation between this ratio and the length of the valley. The ratio of basin areas, R_a, and of stream lengths, R_l, may be similarly affected. This is illustrated in Figure 4.

Hack's Law

The next step in the analysis is examining the relationship between stream length and drainage area in each of the networks. Logarithmic plots of these values for all sub-basins of order greater than 1 are shown in Figure 5 a-h. The Orange river plot has by far the most data points (4098), and the power-law relation (linear on a log-log plot) is obvious. The slope, corresponding to the value of h is 0.685 ± 0.004, *i.e.* clearly not 0.5. The correlation coefficient is high (92.5 %), but it should be noted the graph is slightly concave. The Limpopo plot gives h = 0.642 ± 0.008, with a correlation coefficient of 92.7 %. The smaller network only gave 1030 data points, but the power law relation is clearly seen, as is the slight concavity of the curve. The 6 Cape Fold Belt rivers had much fewer data points than the two big rivers: the largest of the 6, the Olifants, had 204 sub-basins of order 2 and above, while the Kei had just 45. Nonetheless, Hack's Law plots for these basins are all very well correlated, and give values of h between 0.585 and 0.665, with the uncertainties varying between 0.018 and 0.032 in each case. As was the case with the Orange and Limpopo, the slope is not constant in these graphs, but decreases with increasing area. As the slope of the logarithmic plots corresponds to the value of h, any changes in it imply that the exponent's value is not constant. Thus from the data presented here it is clear that h varies not only between basins, but also with scale in each basin, confirming the existence of scaling regimes.

Short Range and Randomness Regimes

The plots in Figure 5 suggest that two scaling regimes are present in the data obtained from the DEM. The 1 km horizontal resolution is too coarse to identify the hill slope regime – this is confirmed by the fact that the slope of the plots is never equal to 1. At the other end of the scale, dealing with drainage of a relatively small

Table 1. Horton's ratios for the river networks of southern Africa

	ω	$n(\omega)$	$R_n(\omega)$	$l(\omega)$ [km]	$R_l(\omega)$	$a(\omega)$ [km^2]	$R_a(\omega)$
Orange	2	3,195	4.64	19.6	3.01	188	4.83
	3	689	4.28	59.2	2.48	908	4.44
	4	161	4.13	146	2.01	4,030	3.87
	5	39	3.9	294	2.17	15,600	4.92
	6	10	3.33	637	1.52	76,700	2.75
	7	3	3	970	2.22	211,000	4.93
	8	1		2,150		1,040,000	
Limpopo	2	830	5.29	22	3.06	262	5.67
	3	157	4.76	69	2.67	1490	5.49
	4	33	4.71	183	1.94	8140	3.81
	5	7	3.5	354	2.81	31100	6.14
	6	2	2	995	1.52	191000	2.02
	7	1		1510		386000	
Olifants	2	157	4.24	21	2.76	246	4.71
	3	37	5.29	58	2.05	1160	2.95
	4	7	3.5	119	3.88	3420	10.67
	5	2	2	462	1.24	36500	2.02
	6	1		572		73800	
Gourits	2	110	5.24	22	2.5	272	4.45
	3	21	3.5	55	2.64	1210	5.52
	4	6	3	145	1.63	6680	3.85
	5	2	2	236	1.4	25700	2.09
	6	1		330		53700	
Gamtoos	2	88	5.18	23	2.65	261	4.87
	3	17	8.5	61	4.08	1270	9.76
	4	2	2	249	2.02	12400	3.31
	5	1		502		41100	
Sundays:	2	41	3.73	24	2.38	381	3.02
	3	11	5.5	57	1.67	1150	3.38
	4	2	2	95	3.65	3890	6.81
	5	1		347		26500	
Great Fish	2	70	4.67	21	2.62	300	3.77
	3	15	3.75	55	1.69	1130	2.83
	4	4	4	93	5.41	3200	11.38
	5	1		503		36400	
Kei	2	34	4.25	23	2.78	360	4.39
	3	8	4	64	1.78	1580	3.06
	4	2	2	114	2.55	4830	4.74
	5	1		291		22900	

section of a continent will not provide much data that could represent the maximal basins bound by continental-scale structures. We thus conclude that the graphs on Figure 5 show the two regimes in the middle of the scale of Dodds and Rothman (2000), *i.e.* short-range and randomness, and that the basin size at which the slope changes corresponds to the cross-over between them.

As the Orange drains different terains, data will be lost unless the network is separated into smaller sub-networks. The 6 networks discussed earlier, and shown in Figure 1 (Vaal, Upper Orange, Molopo, Nossob, Fish and Hartebees) were thus treated separately here. Similarly, the Limpopo data was separated into two smaller networks – the Elands, and the upper Limpopo (upstream from the Elands confluence). This provided 14 basins for the analysis, their properties summarized in Table 2. In the table, D corresponds to the fractal dimension of the topography over which the network flows, and R the roughness of this topography. Both these parameters are computed using the spectral techniques of Turcotte (1992). The uncertainty associated with the mean slope of sub-basins in a given network appears to be large, but this is not unexpected – each network contains many steep streams, as well as many gentle ones, so the standard deviation of these slopes is the same order as their mean.

Correlation coefficients between h and basin parameters included in Table 2 were calculated. While the fractal dimension of the topography was observed to have no influence on the resulting Hack's exponent (correlation of 22.2%), there was strong negative

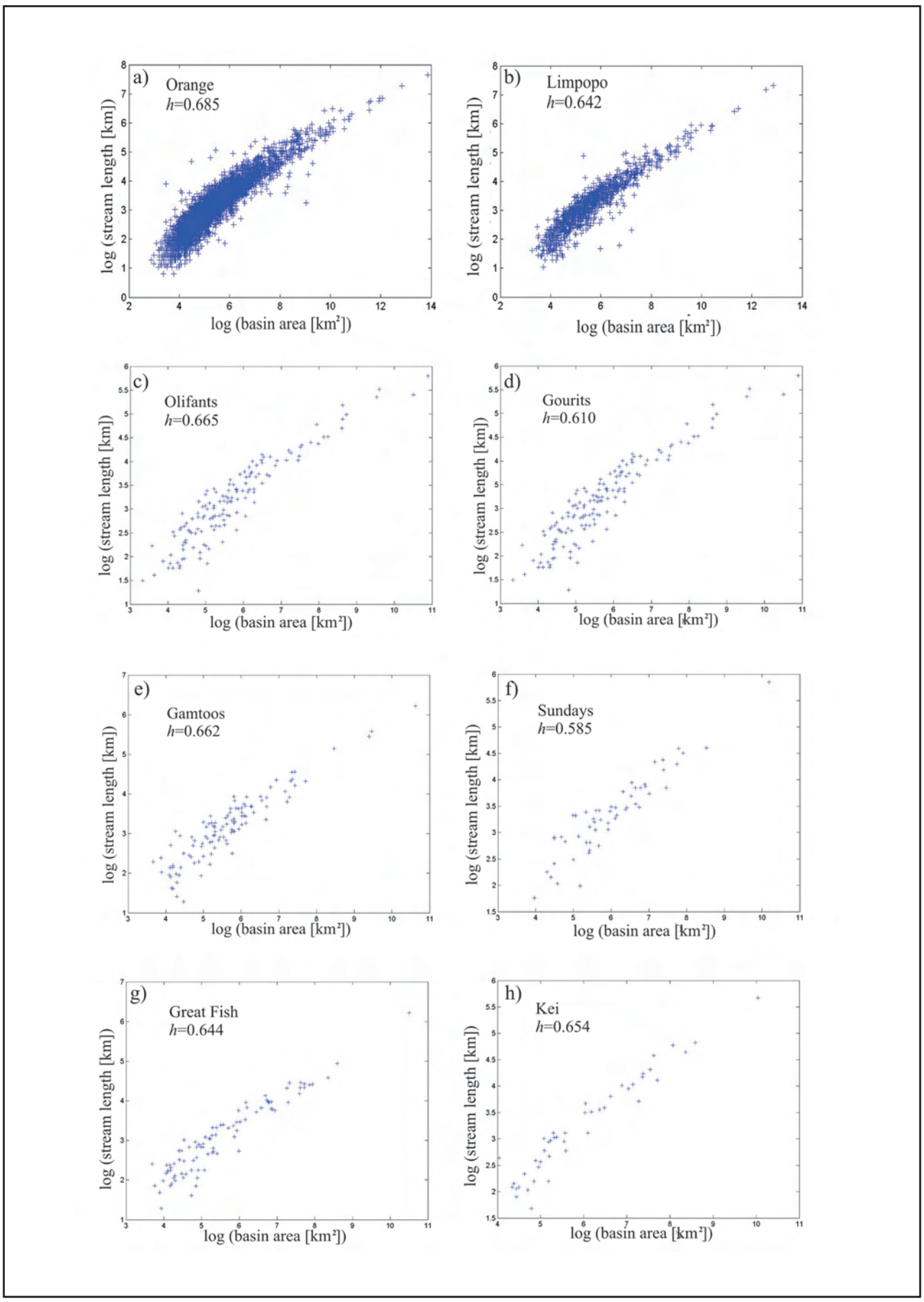

Figure 5. (**a-h**) Hack's Law plots for the eight networks included in the study. The exponent's value in each network is shown in the graph.

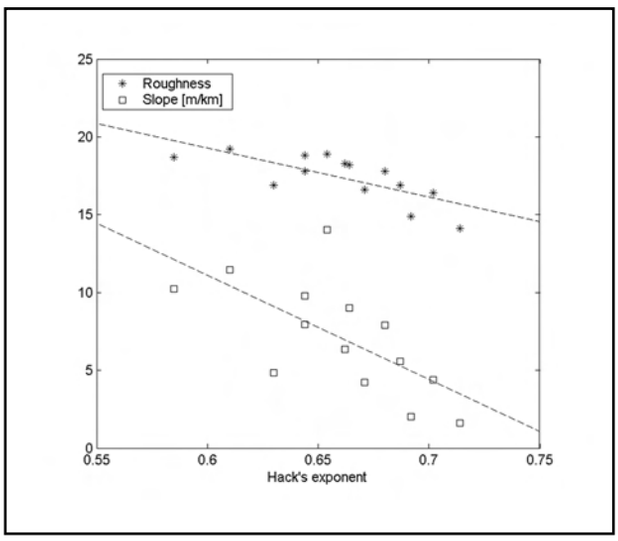

Figure 6. Topography roughness and mean sub-basin slope of each of the 14 basins plotted on a combined y-axis against Hack's exponent of the corresponding networks. Regression lines have been drawn for each parameter to show the strong inverse correlations.

correlation between h and each of mean sub-basin slope and topography roughness (correlation of -66.3% and -73.6%, see Figure 6). For 14 data points, with these correlation coefficients a direct relationship between the parameters in question can be stated with 99% confidence. One would expect topography roughness and mean basin slope to be closely correlated, and therefore have similar correlation with other parameters. Thus in rough areas, where basins are relatively steep, the value of h for the combined short-range and randomness regimes is lower than in smoother landscapes with gently sloping river basins.

The next step in the analysis is to separate the two regimes from each other. To do this a statistical analysis was performed. From the Hack's Law plots (Figure 5) one can see the threshold between the two regimes is somewhere between values of 5 and 8 for the logarithm of basin area. For each basin this threshold was varied between these values in steps of 0.01, and the ordered pairs separated into two sets. The slope of the logarithmic plot, corresponding to h, and the slope uncertainty was computed for basins on either side of the threshold value. The threshold value for which the average of the two slope uncertainties was smallest was assumed to represent the real threshold for that particular network. These thresholds, as well as values for h and their uncertainties for basins in each regime, are given in Table 3. These values were then compared with the properties of the topography that the river basin drains: mean slope, roughness and fractal dimension (included in Table 2). As with the overall value for h, the fractal dimension has no correlation with the exponent. The roughness presents an interesting picture (Figure 7): the short-range regime data shows an inverse correlation between h and the roughness (correlation coefficient of 80.1%, so the regression can be stated with 99% confidence). The randomness regime, made up of sub-basins with drainage areas above the given threshold, shows a weak positive regression between h and the roughness. The correlation coefficient here has a much lower value of 32.6%, which puts it outside the 90% confidence interval. It is interesting that the values of h in the randomness regime are mostly between 0.5 and 0.6, with an average of 0.55. When we recall that d usually fluctuates between 1.0 and 1.2, with a typical value of 1.1 (eq. 4), it is possible that basins in this regime approach self-similar shapes ($D = d/h = 2$). To verify this suggestion it would be necessary to investigate the variations in d for these basins – this is beyond the scope of this study, but is certainly worth pursuing. The correlations of h with slope are similar, but weaker than ones with roughness, as was the case with entire basins (Figure 6). The plot of the best-fit threshold as a function of topography roughness is shown in Figure 8. The parameters seem independent of each other, though the three basins with the smoothest topographies (Nossob, Molopo and Vaal) also have the thresholds at smallest areas.

Table 2. Parameters of networks examined in this study. Basin area in sq. km, slope in m/km

River	log (a)	b	mean sub-basin slope	D	R
Vaal	12.0	0.702 ± 0.011	4.41 ± 2.90	2.18 ± 0.27	16.4 ± 1.28
Upper Orange	11.5	0.644 ± 0.015	7.94 ± 6.78	2.31 ± 0.15	17.8 ± 1.49
Hartebeest	11.6	0.671 ± 0.012	4.22 ± 2.45	2.22 ± 0.19	16.5 ± 1.58
Fish	11.6	0.687 ± 0.012	5.56 ± 4.15	2.24 ± 0.19	16.9 ± 1.73
Nossob	12.1	0.714 ± 0.012	1.60 ± 1.47	2.30 ± 0.25	14.1 ± 1.66
Molopo	11.9	0.692 ± 0.010	2.03 ± 1.60	2.13 ± 0.23	14.9 ± 1.96
Olifants	11.2	0.664 ± 0.018	9.02 ± 7.64	2.24 ± 0.18	18.2 ± 1.61
Gourits	10.9	0.610 ± 0.021	11.44 ± 8.31	2.16 ± 0.20	19.2 ± 1.54
Gamtoos	10.6	0.662 ± 0.027	6.35 ± 4.15	2.22 ± 0.19	18.3 ± 1.26
Sundays	10.2	0.585 ± 0.032	10.24 ± 621	2.21 ± 0.17	18.7 ± 1.25
Great Fish	10.5	0.644 ± 0.024	9.80 ± 6.29	2.25 ± 0.15	18.8 ± 1.18
Kei	10.0	0.654 ± 0.029	14.03 ± 10.05	2.29 ± 0.16	18.9 ± 0.93
Elands	11.5	0.680 ± 0.016	7.91 ± 7.54	2.19 ± 0.20	17.8 ± 1.78
Upper Limpopo	12.0	0.630 ± 0.010	4.86 ± 3.15	2.17 ± 0.21	16.9 ± 1.36

Table 3. Hack's exponent for basin on either side of the best-fit threshold. Threshold given as log (area in sq. km)

Basin	h (short range)	h (random)	area threshold
Vaal	0.811 ± 0.021	0.583 ± 0.022	6.19
Upper Orange	0.683 ± 0.026	0.586 ± 0.029	6.61
Hartebeest	0.751 ± 0.017	0.510 ± 0.023	7.30
Fish	0.776 ± 0.019	0.549 ± 0.026	6.72
Nossob	0.881 ± 0.027	0.523 ± 0.027	5.79
Molopo	0.819 ± 0.021	0.509 ± 0.021	6.23
Olifants	0.688 ± 0.036	0.579 ± 0.032	6.45
Gourits	0.726 ± 0.043	0.481 ± 0.030	6.55
Gamtoos	0.687 ± 0.043	0.565 ± 0.043	7.29
Sundays	0.576 ± 0.066	0.572 ± 0.061	6.75
Great Fish	0.686 ± 0.035	0.659 ± 0.039	7.33
Kei	0.689 ± 0.054	0.538 ± 0.067	7.28
Elands	0.757 ± 0.024	0.543 ± 0.033	7.32
Upper Limpopo	0.671 ± 0.015	0.544 ± 0.026	7.33

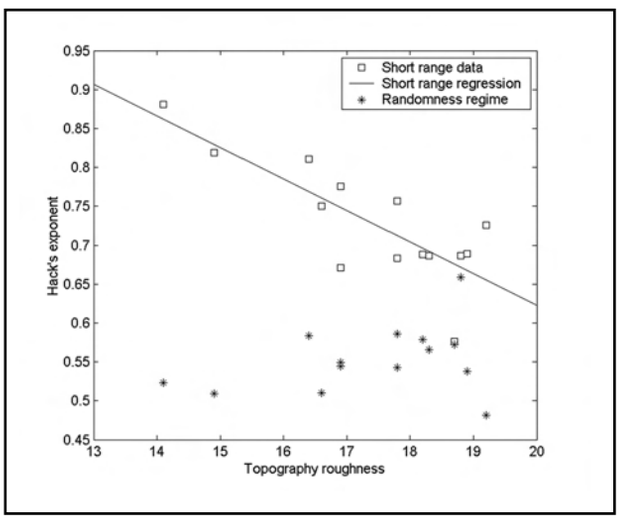

Figure 7. Hack's exponents for the 14 sub-network data separated into the short range regime (squares) and 'randomness' (stars). Regression line of the short range regime results shows the strong inverse correlation, while random regime results are independent of roughness.

We therefore conclude that in the short-range regime the scaling parameter h is dependant on the roughness of the topography – at smaller scales it is negatively correlated with the roughness. When basin reach the size of a certain threshold (around 400 km^2 in very smooth topographies, but often over 1000 km^2), a new regime is entered and a weak positive regression is observed. This latter regression in not conclusive, and there is a possibility of basins in that regime being self-similar. As the short-range regime contains more data points than the randomness one, when the 2 regimes are combined (Figure 6) the prevailing trend is that of the short-range regime.

Hill-slope Regime

As was mentioned earlier, the DEM resolution was not sufficient to study the hill-slope run-off patterns in linear

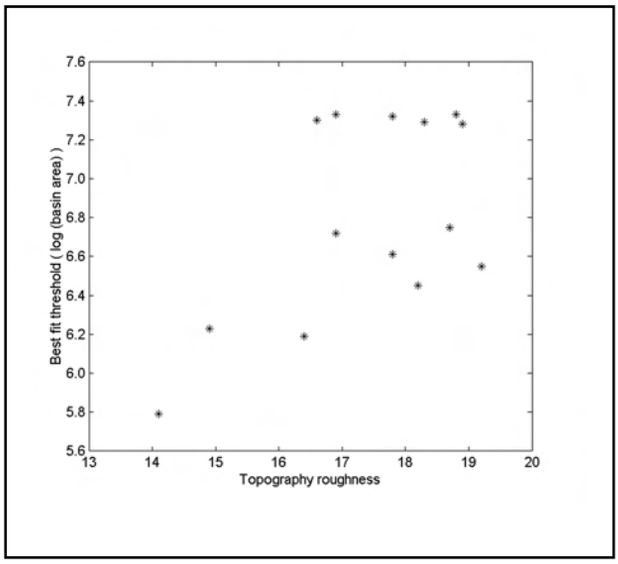

Figure 8. Best-fit area threshold as a function of basin's topography roughness.

mountain belts. Three setting where such drainage can be observed were identified (Figure 9). The Cape Fold Belt (CFB, setting 1) was already discussed, with its schematic drainage shown in Figure 4. Eight individual linear sections were identified there. Similar pattern are observed in the valleys cut into the basalt highlands in Lesotho (setting 2 – eight sections analysed here). The simplified structure of that setting is shown in Figure 10. The figure also shows parallel streams draining setting 3 – linear sections of the Drakensberg Escarpment, where five such sections were identified. It should be remembered that all 21 sections drain the same side of the particular mountain range.

In each locality the mean spacing of adjacent streams (S) was computed. Other parameters were also assembled, such as the mean slope of the drained mountainside. The half-width of the mountain belt (W – defined as the mean distance between the watershed and the trunk stream parallel to it, see Figure 3) and mean height (h) of the watershed above this trunk stream in settings (1) and (2). As the valleys in Lesotho become wider downstream, the mountain belt width is given as a range, as is the watershed's height above the valley. The escarpment drainage on the eastern side of the Drakensberg watershed is a little problematic. What was described as the half-width of ranges in the other settings was impossible to describe or measure here, as there is no convenient trunk stream parallel to the mountain range. All the measurements are presented in Table 4.

From the data in Table 4 one can see there is no suggestive correlation in any setting between spacing in an individual locality and any parameter included in this table. It does, however, appear that the spacing is consistently larger in the CFB than in the other settings. The mean of the 155 spacings in the CFB is 1.86 km, with a standard deviation of 0.74 km. From the Drakensberg escarpment 62 spacings were obtained,

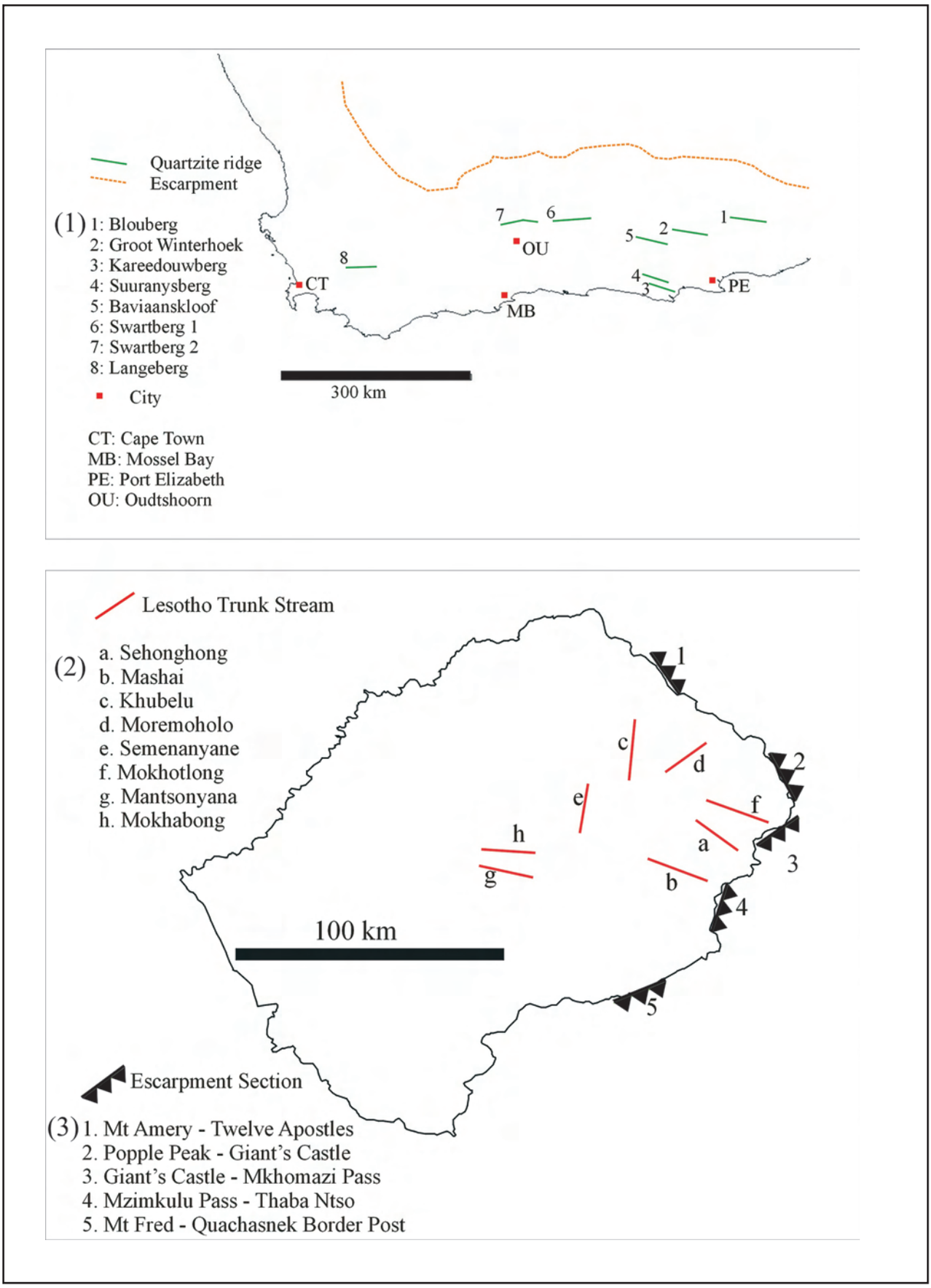

Figure 9. Location of linear mountain belts used in the study. Cape Fold Belt ranges (setting 1) on top, Lesotho Highland streams (setting 2) and linear section of the Drakensberg Escarpment (setting 3) at the bottom. The black curve on the bottom figure marks the border of Lesotho. In the east this coincides with the watershed between headwaters of the Orange and drainage into the Indian Ocean.

Table 4. Linear belt stream spacing parameters. n is the number of spacings at each locality.

Locality	Setting	n	S (km)	slope (m/km)	h (m)	W (km)
Blouberg	CFB	18	1.63 ± 0.47	110	300	2.8
Groot-Winterhoek	CFB	30	1.83 ± 0.51	160	690	4.3
Kareedouwberg	CFB	12	1.90 ± 0.78	140	490	3.5
Suuranysberg	CFB	15	2.20 ± 0.78	160	440	2.7
Baviaanskloof	CFB	20	1.83 ± 0.67	170	890	5.2
Swartberg1	CFB	22	1.75 ± 0.69	160	720	4.5
Swartberg2	CFB	20	2.35 ± 0.96	200	1100	5.5
Langeberg	CFB	18	1.51 ± 0.85	230	620	2.6
Sehonghong	Lesotho	12	1.65 ± 0.38	140	400-1100	3-8
Mashai	Lesotho	14	1.64 ± 0.58	150	300-600	2-4
Khubelu	Lesotho	16	1.48 ± 0.37	140	500-700	4-5
Moremoholo	Lesotho	10	1.55 ± 0.28	140	400-700	3-5
Semenanyane	Lesotho	11	1.39 ± 0.36	130	400-600	3-5
Mokhotlong	Lesotho	13	1.62 ± 0.35	150	600-800	4-5
Mantsonyane	Lesotho	10	1.23 ± 0.34	100	300-500	3-5
Mokhabong	Lesotho	12	1.52 ± 0.49	80	200-400	3-5
Mount Amery	Escarpment	11	1.52 ± 0.63	400		
Popple Peak	Escarpment	11	1.18 ± 0.46	270		
Giant's Castle	Escarpment	13	1.54 ± 0.41	290		
Mzimkulu Pass	Escarpment	15	1.25 ± 0.47	270		
Mount Fred	Escarpment	12	1.52 ± 0.49	150		

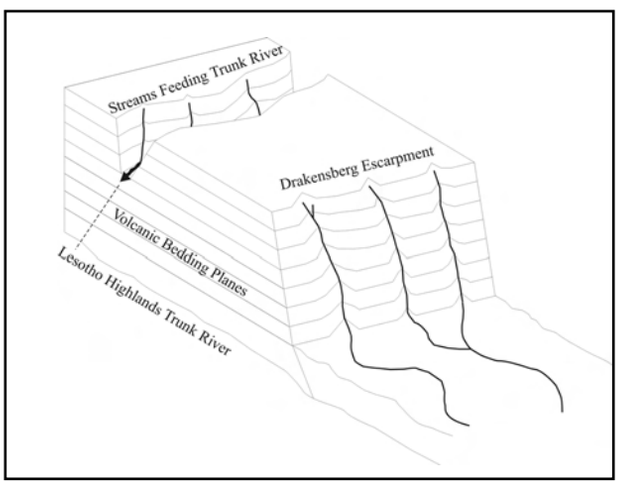

Figure 10. Schematic figure of the two drainage types of the Drakensberg Basalts (see text for further explanation).

their mean being 1.40 km, with a standard deviation of 0.52 km, while the 98 spacings in Lesotho gave a mean value of 1.52 ± 0.41 km. Thus it seems that the spacing of streams in the Lesotho valleys and the Drakensberg escarpment (which have the same underlying rock-type, but different geomorphology) have similar distribution, which is different to that observed in the CFB. Thus the only factor which controls the stream spacing in linear mountain belts is the underlying geology.

The standard deviations associated with these mean spacings seem large. They are, however, similar to the deviations observed at all individual localities (Table 4). As parameters like joint spacing, soil, vegetation and climate cannot be expected to vary significantly on a single side of single mountain range, we must conclude that the variations in the spacing are random. Thus while hill-slope regime of Hack's Law, with the value of the exponent h very close to 1, exists in different mountain settings, there are considerable random fluctuations around this distribution. Furthermore, the constant, c, in the equation (2) is determined by regional rock-type of the mountains concerned.

Discussion

Our analysis of river basins in southern Africa showed that while river networks can be described in terms of fractal patterns, there exists a large amount of deviation around these patterns. While some of these deviations can be explained in terms of geological phenomena (such as unusually high Horton's ratios in parallel mountain belts), others do not have obvious explanations.

One of the most commonly parameters used to quantify network geometry is Hack's exponent, h, which relates drainage area to stream length. This exponent was measured for 14 networks in southern Africa, and significant differences in its value were observed in separate basins. Strong inverse correlation of h with the roughness of the topography, as well as with mean sub-basin slope, was observed. There were, however, significant deviations from these regressions. The Sundays and Great Fish rivers, which drain very similar terrains right next to each other and have virtually the same roughness, had very different values of h: 0.585 and 0.644. We cannot offer an explanation for similar basin having significantly different network parameters, and conclude these, and other differences, are results of randomness. Alternatively, the difference could be the result of small variations in initial conditions of basin formation. If formation of river networks is a complex

system, and the existence of power laws and thresholds suggests that it might be, infinitesimal initial differences could potentially lead to vastly different results as the system evolves.

We proceeded to investigate how h changes with scale. We based our analysis on the scaling regime hypothesis of Dodds and Rothman (2000), which proposes the existence of four regimes. At the smallest scales one expects parallel non-convergent streams flowing down hill slopes. In this case one expects h to be close to 1, if the basin width remains uniform. This regime can be best analysed in linear mountain belts, examples of which can be found in the Cape Fold Belt, Lesotho Highlands, and Drakensberg Escarpment. We found that separation of these streams (corresponding to basin width) depends on the underlying rock type and/or structure (*e.g.* joint patterns). Once again, there were significant deviations associated with the distribution of basin width, which presently we can only attribute to randomness.

Once streams begin to converge, a regime termed 'short range' is entered, and at even larger scales the existence of 'randomness' regime has been hypothesised. Our results showed a clearly visible threshold between these regimes. The exact position of this threshold varied between basins – in ones with smooth topography it is as low as 400 km^2, but in others over 1000 km^2. Hack's exponent for the sub-basins smaller than the threshold (short range regime) are very strongly inversely correlated with roughness of the topography, while the larger ones (randomness regime) appear independent of roughness, and mostly had values of h between 0.5 and 0.6. These values correspond to self-similar basin shapes, but a detailed analysis of individual streams' fractality is necessary before any robust conclusions can be made. As there are many more basins in the short-range than the randomness regime, the h-roughness correlation for the combined data is inherited from the stronger h-roughness relationship in the short-range regime.

The hypothesis of Dodds and Rothman (2000) suggests a fourth regime of continental scale basins, which these authors suggest would be self similar. Our presented study area is not large enough to study continental-scale rivers, but it is very interesting to note that our randomness regime basins could be self-similar, and may therefore be part of the maximal, continental regime. Southern Africa is a unique section of a tectonically unique continent (Holmes, 1965; Doucouré and de Wit, 2003), and it should not be surprising if mechanism responsible for the formation of its basins were different than those on other continents. A continental scale analysis of African rivers is in preparation.

Acknowledgements

We would like to thank Prof. Dan Rothman, who generously shared his knowledge on river network geometry, and made it possible for J.S. to enjoy an extended stay at MIT. Dr Mike de Wit, of de Beers Consolidated Mines Ltd, supplied us with a database of African river networks. We benefited from valuable discussions with him as well as with Moctar Doucouré and Woody Cotterill. The manuscript benefited greatly from constructive reviews by Brian Bluck and an exceptionally detailed analysis by Tom Blenkinsop. The work was financed through the South African National Research Foundation.

References

Bootsman, C.S. (1997). On the Evolution of the Upper-Molopo Drainage. *South African Geographical Journal*, **79**, 83-92.

Buckle, C. (1978). Landforms in Africa: An Introduction to Geomorphology. *Longman Group, Essex, England*, 249pp.

Cox, K.G. (1989). The role of mantle plumes in the development of continental drainage patterns. *Nature*, **342**, 873-877.

de Wit, M.C.J. (1993). Cainozoic Evolution of Drainage Systems in the North-Western Cape. *Unpublished PhD thesis, University of Cape Town, South Africa*, 371pp.

Dodds, P.S. and Rothman, D.H. (1999). Unified view of scaling laws for river networks. *Physics Review E*, **59**, 4865-4877.

Dodds, P.S. and Rothman, D.H. (2000). Scaling, Universality, and Geomorphology. *Annual Review of Earth and Planetary Science*, **28**, 571-610.

Doucouré, C.M and de Wit, M.J. (2003). Old inherited origin for the present near-bimodal topography of Africa. *Journal of African Earth Sciences*, **36**, 371-388.

Hack, J.T. (1957). Studies of longitudinal stream profiles in Virginia and Maryland. *US Geological Survey Professional Paper,* **294B**, 45-97.

Holmes, A. (1965). Principles of Physical Geology. (2nd edition). *William Clowes and Sons, London*, 1288pp.

Horton, R.E. (1945). Erosional development of streams and their drainage basins; hydrophysical approach to quantitative morphology. *Bulletin of the Geological Society of America,* **56**, 275-370.

Maritan, A., Rinaldo, A., Rigon, R., Giacometti, A. and Rodriguez-Iturbe, I. (1996). Scaling laws for river networks. *Physics Review E*, **53**, 1510-1515.

Mueller, J.E. (1973). Re-evalueation of the relationship of master streams and drainage basins: reply. *Bulletin of the Geological Society of America,* **84**, 3127-3130.

Reeves, C.V. (1972). Rifting in the Kalahari? *Nature*, **237**, 95-96.

Reeves, C.V. (1978). A failed Gondwana spreading axis in southern Africa. *Nature*, **273**, 222-223.

Rigon, R., Rodriguez-Iturbe, I., Maritan, A., Giacometti, A., Tarboton, D.G. and Rinaldo, A. (1996). On Hack's Law. *Water Resources Research*, **32**, 3367-3374.

Rigon, R., Rodriguez-Iturbe, I. and Rinaldo, A. (1998). Feasible optimality implies Hack's Law. *Water Resources Research*, **34**, 3181-3189.

Rodriguez-Iturbe, I. and Rinaldo, A. (1997). *Fractal River Basins: Chance and Self-Organization*. Cambridge, UK: Cambridge University Press, U.K., 547pp.

Shreve, R.L., (1967). Infinite topologically random channel networks. *Journal of Geology*, **75**, 178-186.

Stankiewicz, J. (2004). African river basins: their present geometry and recent past as a framework for their evolution. *Unpublished PhD thesis, University of Cape Town, South Africa*, 229pp.

Stankiewicz, J. and de Wit, M.J. (2005). River Networks of Southern Africa – Scaling Laws governing their geometry and deviations from scaling. *Geochemistry, Geophysics, Geosystems (G^3)*. In press.

Strachler, A.N. (1957). Quantitative analysis of watershed geomorphology. *EOS Transactions, American Geophysical Union,* **38**, 913-920.

Turcotte, D.L. (1992). Fractals and chaos is geology and geophysics. *Cambridge University Press, U.K.*, 221pp.

White, R. and McKenzie, D. (1989). Magmatism at rift zones: The generation of volcanic continental margins and flood basalts. *Journal of Geophysyical Research,* **94**, 7685-7729.

Editorial handling: J. M. Barton